

Modeling of heat transfer in tanks during wine-making fermentation

Sophie Colombié *, Sophie Malherbe, Jean-Marie Sablayrolles

INRA-UMR Sciences pour L'œnologie, 2 Place Viala, 34060 Montpellier cedex 1, France

Received 25 November 2005; received in revised form 23 May 2006; accepted 26 May 2006

Abstract

Temperature is one of the main factors that affect the fermentation kinetics during wine-making. We developed a thermal model to evaluate the power required to control this temperature. The model includes the changes in physico-chemical properties of the must during fermentation and the refrigeration losses to ambient from the outer surface of the tank. We used the model to run simulations and to estimate the power required to cool an industrial tank. The results were discussed considering the impact of variables such as the air speed and the air temperature. We finally validated the thermal model at the pilot scale.

© 2006 Elsevier Ltd. All rights reserved.

Keywords: Heat transfer; Model; Wine-making fermentation

1. Introduction

There have been many attempts to develop mathematical models of heat transfer (Le Roux, Purchas, & Nell, 1986; Lopez & Secanell, 1992; Varma, 1999) including those appropriate for wine-making fermentations (Boulton, 1980). However, the conditions for which they have been validated are too restricted for them to be usable in practice.

There are various difficulties associated with developing a thermal model:

- (1) The changes of physico-chemical properties of the must during alcoholic fermentation in tanks. Manzocco, Maltini, and Lerici (1998) studied these properties using a simplified experimental model simulating the fermentation of a 25% sugar–water mixture into a 12.78% ethanol–water mixture. They showed that there are large thermal and physical changes associated with the steps of fermentation

process (particularly an increase in ethanol vapor pressure, and decreases in water activity and viscosity).

- (2) The hydrodynamic conditions inside tanks:
 - The birth and ascension of CO₂ bubbles during the process. These bubbles have a mechanical role of stirring and affect heat diffusion.
 - Possible temperature gradients. Such gradients can appear (Guymon & Crowell, 1977) but they are usually limited to red wine-making.
- (3) The heterogeneity of industrial tanks (geometry, material, cooling system) and their location (indoors or outside with diverse temperatures and air speeds).

We aimed to develop a simulation model of the thermal behavior of wine-making fermentations. This model will be used to evaluate the power required to cool the tank during fermentation. We previously developed a kinetic model of fermentation able to predict the fermentation kinetics, including anisothermal conditions and nitrogen additions (Malherbe, Fromion, Hilgert, & Sablayrolles, 2004). The kinetic model has been validated in very diverse enological conditions (Colombié, Malherbe, & Sablayrolles, 2005). Thus, it can be integrated into a new control system for

* Corresponding author. Tel.: +33 4 99 61 20 54; fax: +33 4 99 61 28 57.
E-mail address: colombie@ensam.inra.fr (S. Colombié).

wine making, to optimize for example the use of tanks and the total energy required.

The aim was therefore to model the heat transfer in tanks during fermentation process, taking into account the changes of the properties of the must during the process, and to estimate refrigeration losses to the environment from the outer surface of the tank.

We first studied the relationships between the main parameters and the overall heat transfer coefficient U . These parameters were (i) properties of the tank, (ii) convection coefficients at the inside and outside surfaces of the tank, h_i and h_e and (iii) the environment, including air temperature and air speed.

We then ran simulations for large-scale fermentations and finally validated this model with a specific fermentation experiment at the pilot scale (100 L).

2. Model development

We assumed that:

- The must is homogeneous during most of the fermentation.
- The radiation heat transfer is negligible.
- The conduction heat transfer is also negligible.

Tanks commercialized and used have very diverse sizes and geometries. However, for this study, the tank was presumed to be a vertical cylinder; the exchange area (A) was therefore the sum of the area of the wall around the cylinder plus the area of the bottom:

$$A = 2\pi rH + \pi r^2 \quad (1)$$

where H is the height of must in the tank and r is the radius of the tank (the thickness being negligible).

The transient equation for the conservation of the power in the reactor can be written:

$$P_{\text{accumulation}} = P_{\text{fermentation}} + P_{\text{wall}} + P_{\text{evaporation}} + Q_c \quad (2)$$

where $P_{\text{accumulation}}$ is the power accumulated by the must, $P_{\text{fermentation}}$ the power generated by the fermentation, P_{wall} the power exchanged by the walls of the tank, $P_{\text{evaporation}}$ the power lost by evaporation of water and ethanol and Q_c the power required to cool the tank, also called frigories. These last three powers represent the power dissipated to the surroundings. All these expressions are detailed below.

2.1. Power accumulated by the must

During fermentation in tanks, when the temperature is not controlled, the power accumulated by the must due to the heat generated by the fermentation process follows the expression:

$$P_{\text{accumulation}} = 10^{-3} \rho_{\text{must}} V C_{p_{\text{must}}} \frac{dT}{dt} \quad (3)$$

where ρ_{must} is the must density, V the must volume, $C_{p_{\text{must}}}$ the specific heat of the must in fermentation and dT/dt the rate of change of must temperature with time.

The main physicochemical properties of the must and wine have been described in the literature. The thermal capacity has been estimated ($886 \text{ cal kg}^{-1} \text{ }^\circ\text{C}^{-1}$) for a must with 200 g L^{-1} of sugar and for the corresponding wine ($866 \text{ cal kg}^{-1} \text{ }^\circ\text{C}^{-1}$) (MatéVi). We used a linear expression based on these values:

$$C_{p_{\text{must}}} = 0.1 * (S_0 - 2.17 * \text{CO}_2) + 866 \quad (4)$$

where S_0 is the initial sugar concentration in the must and CO_2 the carbon dioxide produced.

The must density depends on the progress of the fermentation and the must temperature as follows (El Haloui, Picque, & Corrieu, 1987):

$$\rho_{\text{must}} = -1.085 * \text{CO}_2 + 0.405 * S_0 - 0.031 * T + 996.925 \quad (5)$$

In most models, the must was assimilated to water but this can lead to an overestimation of the product $\rho_{\text{must}} C_{p_{\text{must}}}$ by between 5% and 15%.

2.2. Power generated by the fermentation

Alcoholic fermentation is an exothermic reaction. We used the value for heat production by the reaction as determined by Bouffard (1895) (23500 cal per mole of sugar consumed). Although this value is open to discussion (see Williams, 1982 for a detailed review), it can still be considered as the most accurate available. In view of the relationship between sugar consumed and CO_2 produced in wine making conditions (El Haloui et al., 1987) the power generated by the fermentation in tanks is

$$P_{\text{fermentation}} = \frac{23500 * 2.17}{180} V \frac{d\text{CO}_2}{dt} \quad (6)$$

where $d\text{CO}_2/dt$ is the CO_2 production rate.

2.3. Power exchanged through the tank wall

Heat convection equations with the associated boundary conditions are required to calculate the power exchanged by the tank walls

$$P_{\text{wall}} = 10^{-3} UA(T - T_e) \quad (7)$$

$$\text{with } U = \frac{1}{\frac{1}{h_i} + \frac{1}{h_e} + \frac{e}{\lambda}} \quad (8)$$

U is the overall heat transfer coefficient, T_e the air temperature, h_i and h_e the convection coefficients at the inside and the outside surface of the tank respectively, e the thickness of the tank material and λ the thermal conductivity of the tank material.

There are at least two main mechanical actions leading to convection inside the tank: (1) heat diffusion in the must

and (2) CO₂ bubble ascension and Brownian phenomena in the must. Bubble ascension is particular because bubbles are produced everywhere throughout the reactor (at all levels) during fermentation of a must with changing characteristics. This type of system has not been described, but can be compared to air bubbles during ebullition of liquids or air injection into a reactor. Mathematical expressions have been written to describe heat transfer in these cases, but these equations require a dimensional numbers to be estimated (Reynolds, Prandtl and Nusselt). Unfortunately, the physicochemical properties of musts required for these equations (viscosity, density, thermal conductivity and heat capacity) are poorly described in the literature.

We used the value determined in enological conditions (Singh, 1982) for the convection coefficient at the inside surface of the tank (h_i). This value varies with the nature of the must and the mechanical stirring in the tank but the impact of such variations on the heat balance is negligible (see below).

To estimate the convection coefficient outside the tank (h_e), two cases have to be considered: (i) natural convection when the air flux, due to the change of density near the wall, is vertical and (ii) forced convection when the air flux is horizontal and fast, that is the case for tanks in ventilated rooms or tanks outdoors.

Whether the convection is natural or forced, the convection coefficient is calculated from the Nusselt number (Nu) as follows:

$$h_e = \frac{Nu \lambda_{\text{air}}}{H} \quad (9)$$

where λ_{air} is the thermal conductivity of air.

Case (1): forced convection

We used an empirical relation (from various experimental results) reported by Mc Adams (1954) to evaluate the convection coefficient of air flowing around a cylinder kept at constant temperature:

$$Nu = 0.32 + 0.43Re^{0.52} \quad (10)$$

with the Reynolds number Re :

$$Re = \frac{s_{\text{air}} 2r}{\nu_{\text{air}}} \quad (11)$$

s_{air} is the air speed and ν_{air} is the kinematic viscosity of air.

All the physical properties of air generally remain constant within the temperature range used in enological conditions. The model thus assumes that they are constant (values determined at 20 °C, Perry's Chemical Engineer's Handbook).

Case (2): natural convection

We used the expression reported by Lienhard (2000) to evaluate the Nusselt number:

$$Nu = 0.678Ra^{1/4} \left(\frac{Pr}{0.952 + Pr} \right)^{1/4} \quad (12)$$

where Ra is the Rayleigh number and Pr the Prandtl number given by the following expressions:

$$Ra = \frac{g \left(\frac{1}{273.15 + T_e} \right) (T_e - T) H^3}{\nu_{\text{air}} \alpha_{\text{air}}} \quad (13)$$

and

$$Pr_{\text{air}} = \frac{\nu_{\text{air}}}{\alpha_{\text{air}}} \quad (14)$$

g being the gravity constant and α_{air} the thermal diffusivity of air.

2.4. Power lost by evaporation of water and ethanol

There have been various works on power losses through evaporation, some a very long time ago (Dubrunfaut, 1856; Bouffard, 1895). Findings for rates of ethanol evaporation are divergent (from 0.083% to 1.36%) depending on experimental conditions. Williams and Boulton (1983) measured the effect of several variables (inoculation rate, sugar concentration, must temperature and air temperature in the headspace of the reactor) on the rate of ethanol evaporation. However, their model was not sufficiently accurate, especially for the early stages of fermentation. Vannobel (1988) suggested (i) a theoretical model validated on semi-empirical and empirical data and based on Raoult and Dalton laws and (ii) a more pragmatic model used here to calculate the power lost by evaporation:

$$P_{\text{evaporation}} = \frac{0.2233V \frac{d\text{CO}_2}{dt} \left(2 + \frac{10.85\text{CO}_2}{1514.19 - 0.95(s_0 - 2.17\text{CO}_2)} \right) 1.0592^T}{270.92 - \left(2 + \frac{10.85\text{CO}_2}{1514.19 - 0.95(s_0 - 2.17\text{CO}_2)} \right) 1.0592^T} \quad (15)$$

The equation for conservation (2) can now be used to run simulations to evaluate the power required to cool the tank.

3. Simulations

The thermal model was combined with the kinetic model (Malherbe et al., 2004) to run simulations and estimate the power necessary to regulate the temperature of an industrial tank (20 m³). The conditions were: initial must temperature 18 °C, final must temperature regulated at 28 °C, air temperature 20 °C, air speed 1.4 m s⁻¹. Each term of power, $P_{\text{fermentation}}$, $P_{\text{accumulation}}$, P_{wall} (in both cases, i.e. natural and forced convection), $P_{\text{evaporation}}$, T and Q_c are plotted in Fig. 1.

From the beginning of the fermentation and while the temperature remained below the maximum (28 °C), all the power produced by the alcoholic fermentation was accumulated by the must. Once the temperature had to be controlled (28 °C), the power required to cool the tank (Q_c) increases to a maximum and then parallels the profile of the power produced by the fermentation.

As the fermentor size increases, the rate of heat production grows more rapidly than the dissipation rate. At large scale, the power exchanged by the walls of the tank (P_{wall}) is about 8–15% (10% is a satisfactory average value) of the

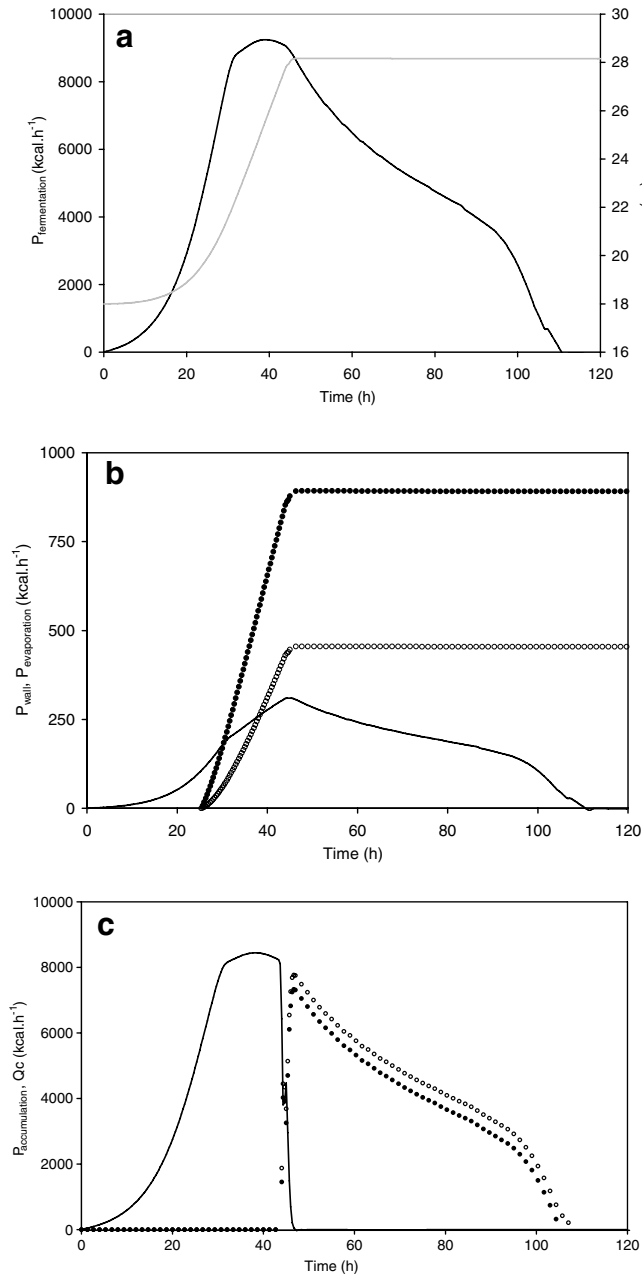


Fig. 1. Simulation of (a) the temperature (T , —) and the power generated by the fermentation process ($P_{\text{fermentation}}$, —), (b) the power exchanged by the walls (P_{wall}) for natural convection (○) and forced convection (●) and the power lost by evaporation ($P_{\text{evaporation}}$, —) and (c) the power accumulated by the must ($P_{\text{accumulation}}$, —) and the power withdrawn by the refrigeration system (Q_c) for both natural (○) and forced (●) convection for fermentation in a tank ($V = 20 \text{ m}^3$, $T_e = 20 \text{ }^\circ\text{C}$, $s_{\text{air}} = 1.4 \text{ m s}^{-1}$) with a must initially containing 0.3 g L^{-1} of assimilable nitrogen and 200 g L^{-1} of sugar.

power produced by the fermentation, and the power lost by evaporation of water and ethanol ($P_{\text{evaporation}}$) is about 4%.

4. Discussion

We assumed that the must is homogeneous thanks to CO_2 bubbles produced during most of the fermentation.

This is usually the case for white-wine making fermentations, and in the liquid phase, below the cap, for red wine-making but, in this case, temperature gradients can create non negligible heat conduction phenomena.

We assumed that the conduction heat transfer is negligible. This assumption is acceptable for polyester tanks and leads to an error of less than 10% for stainless steel tanks (Vannobel, 1988).

Assumptions were required to write equations for convection. Consequently, we studied the impact of the accuracy of different parameters (convection coefficients (h_i and, mostly h_e), tank material and geometry, air speed and temperature) on the overall heat transfer coefficient U . The numerical values used to run the model are listed in the section ‘data used for simulations’.

First, the thickness and the thermal conductivity of the tank material had only a small effect on the coefficient U , whether convection was natural or forced (Table 1). Values of thickness or thermal conductivity ten times higher than those used in the model caused differences of only 3.5% (resp. to 6.6%) in the calculation of U for natural (resp. forced) convection.

The effects of the convection coefficients on the inside and on the outside surfaces of the tank (respectively h_i and h_e) are shown in Fig. 2. The convection coefficient at the inside surface of the tank (h_i) has little effect on U : doubling the value of h_i led to a change in U of less than 3.5%

Table 1

Impact of the thermal conductivity (λ) and the thickness (e) of the tank material on the overall heat transfer coefficient (U) for both natural and forced convection

λ	e	Natural convection U (%)	Forced convection U (%)
λ	$e * 2$	0.6	0.6
λ	$e * 10$	3.5	6
$\lambda/10$	e	3.5	6.6
$\lambda * 15$	e	0.6	0.9

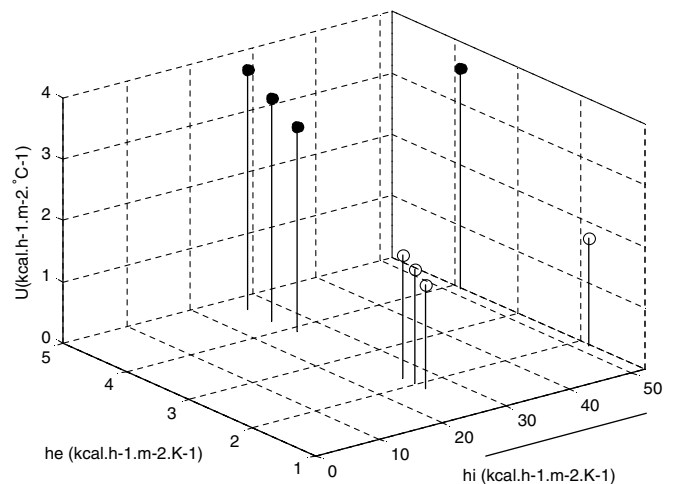


Fig. 2. Impact of convection heat transfer coefficients inside (h_i) and outside (h_e) the tank on the overall heat transfer coefficient (U) for natural (○) and forced convection (●).

for both natural and forced convection. The convection coefficient at the outside surface of the tank (h_e) had a large effect on U : an overestimation of 10% of h_e increased U by 9% for natural and forced convection; and an overestimation of 20% of h_e increased U by 29% for natural convection and 17% for forced convection.

We studied the consequences of differing the parameters of h_e —the air temperature, the air speed and the diameter to height ratio of the tank—on U (Fig. 3). An increase of the air temperature decreased U for natural convection only (Fig. 3(a)). Conversely, an increase of the air speed from 1.4 m s^{-1} (5 km h^{-1}) to 5.6 m s^{-1} (20 km h^{-1}) doubled the value of U , only for forced convection (Fig. 3(b)).

Note that the geometry of the tank, especially the diameter to height ratio, also had a large impact on U in the case of forced convection (Fig. 3(c)). Indeed, for the same volume, the power dissipated by the walls is greater when the tank is wider.

The tank properties (material, geometry and disposition) are usually characteristics which cannot be changed. Nevertheless, the parameters such as the air speed and the air temperature can be variable for tank located inside the winery.

We firstly run simulations in the same conditions than in Fig. 1 but with a periodic variation of the air temperature over 24 h, with an amplitude of $5 \text{ }^\circ\text{C}$ between 15 and $20 \text{ }^\circ\text{C}$ corresponding to temperature changes between the day and the night (Fig. 4(a)). The power exchanged by the wall calculated in the case of forced convection and the frigories (Q_c) were both plotted in Fig. 4(b). The power evacuated by the wall increased and the frigories decreased when the temperature was lower than $20 \text{ }^\circ\text{C}$: Q_c can be lowered by up to 8%.

Then, simulations were run in the same conditions than in Fig. 1 but with a five times higher air speed (7 m s^{-1} , and a constant air temperature $20 \text{ }^\circ\text{C}$). The power exchanged by the wall (forced convection) was almost twice. Consequently the frigories (Q_c) were lowered by 12% (Fig. 4(c)). Thus, in the case of forced convection, the air temperature and—mostly—the air speed can be used as control variables to decrease the power required to cool the tanks inside a cellar. On the contrary, these two variables have a negligible impact on Q_c in the case of natural convection, as indicated on Fig. 3(a) and (b).

To validate the thermal model, we tested it in a fermentation experiment performed at pilot scale.

5. Materials and methods

5.1. Culture conditions

We used the strain *Saccharomyces cerevisiae* K1 ICV-INRA. Fermentations were started with an inoculation of 10^6 cells of active dry yeast per mL. The initial sugar concentration of the must (Carignan variety) was 185 g L^{-1} and the initial assimilable nitrogen concentration was

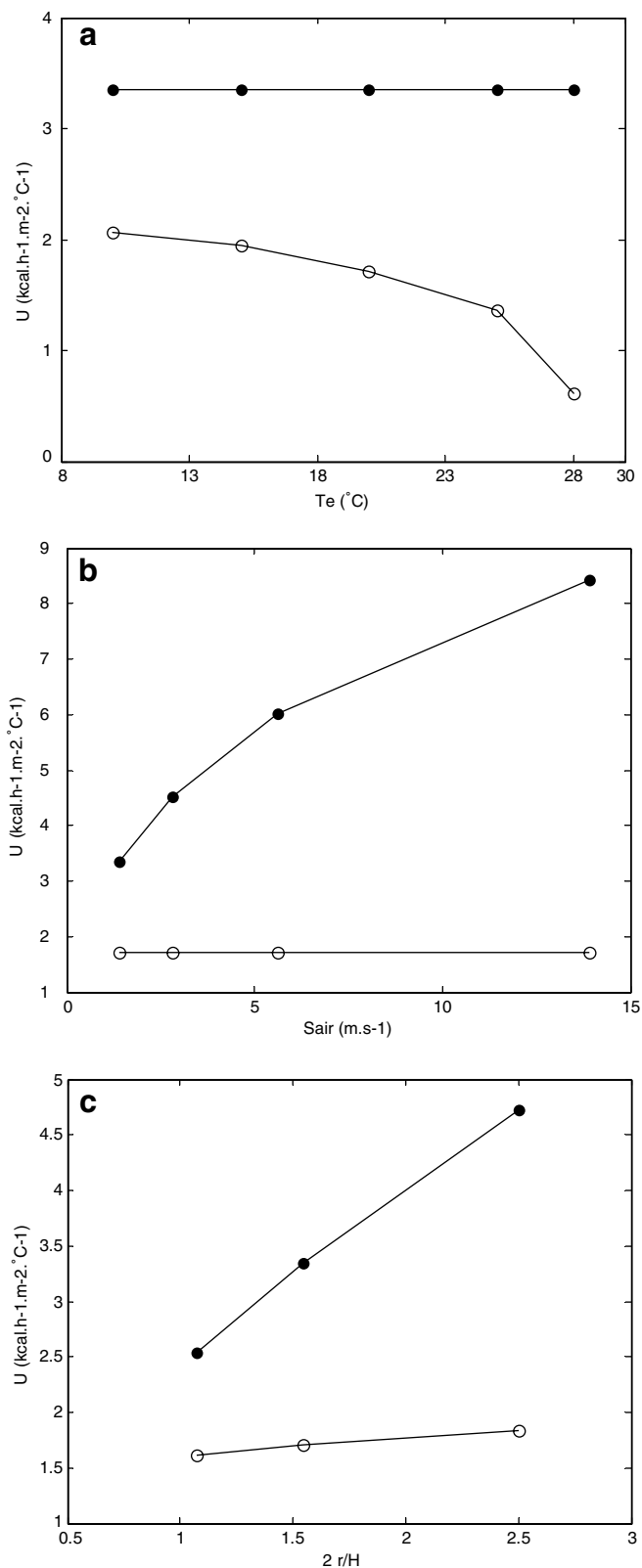


Fig. 3. Impact of (a) the air temperature (T_e), (b) the air speed (S_{air}) and (c) the diameter to height ratio ($2r/H$) on the overall heat transfer coefficient (U) for natural convection (○) and forced convection (●).

0.28 g L^{-1} . Experiments were performed (i) at the laboratory scale in 1.1 l reactors and (ii) at the pilot scale, in

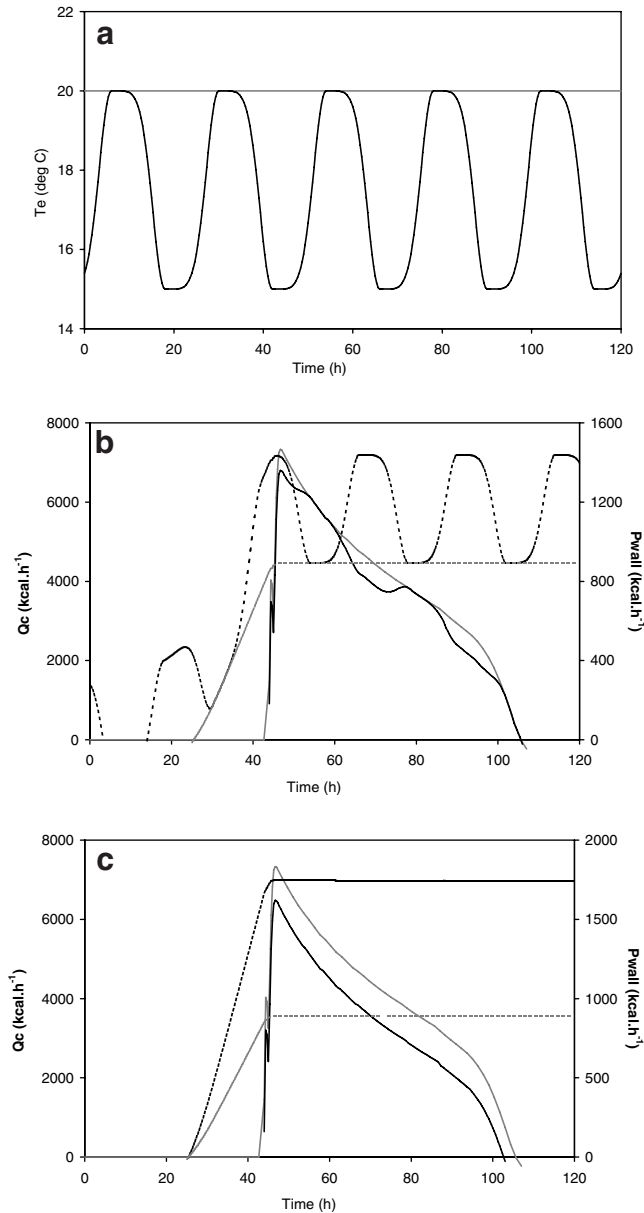


Fig. 4. (a) The air temperature $T_e = 20\text{ }^\circ\text{C}$ (---) and T_e as periodic profile (—). (b) and (c) simulations of the power exchanged by the walls (P_{wall}) (---) and of the power withdrawn by the refrigeration system (Q_c , —) in the case of forced convection (same parameter values than Fig. 1). (b) $T_e = 20\text{ }^\circ\text{C}$ (—) and T_e as periodic profile (—) represented in (a). (c) The air speed $s_{\text{air}} = 1.4\text{ m s}^{-1}$ (---) and $s_{\text{air}} = 7\text{ m s}^{-1}\text{C}$ (—).

100 l stainless steel cylindrical tanks ($r_i = 0.2\text{ m}$; $H = 0.8\text{ m}$, $V = 100\text{ L}$).

5.2. Control of fermentation

At the laboratory scale, the CO_2 release was determined by automatic measurement of bioreactor weight loss every 20 min and the CO_2 production rate was calculated with a high level of precision by polynomial smoothing of the last ten measurements of CO_2 (Sablayrolles, Barre, & Grenier, 1987; Bely, Sablayrolles, & Barre, 1990).

At the pilot scale, the CO_2 production rate was measured on-line by a mass flowmeter. The temperature was measured inside and outside the tank using pt 100 probes.

6. Validation of the heat transfer model

To validate the thermal model, we performed a fermentation with a grape must (Carignan) without temperature control, i.e. with a free temperature profile throughout the fermentation process. The corresponding air and must temperature profiles are reported in Fig. 5, with a polynomial regression fitting (degree 8).

We validated the model using two different methods. We compared:

- (1) the experimental fermentation rate (expressed as the CO_2 production rate) to the predicted fermentation rate calculated from the experimental temperature profile, considering both natural and forced convection (Fig. 6). The shape of the curve of the fermentation rate calculated from the thermal model was close to that determined experimentally on-line. The

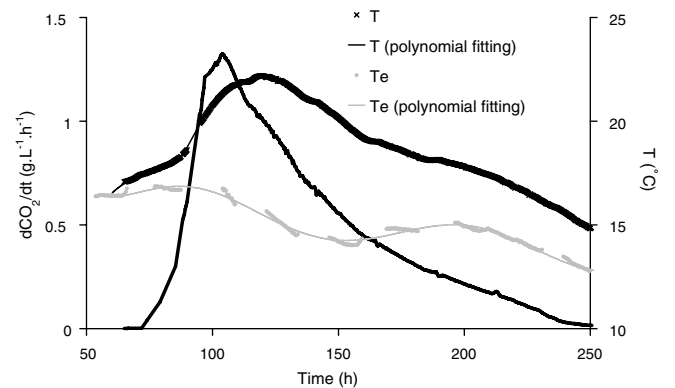


Fig. 5. The fermentation rate ($d\text{CO}_2/dt$, —) the must temperature (T , \times) and the air temperature (T_e , \bullet) during an experiment performed at pilot scale (100 l) without temperature control, with Carignan grape must. Polynomial regressions were used to fit the experimental temperature profiles of must (—) and air (—).

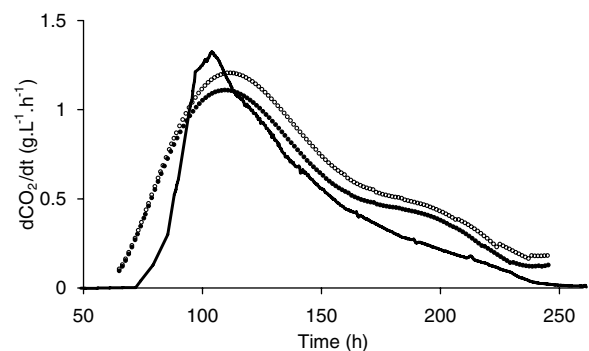


Fig. 6. Simulation of the fermentation rate ($d\text{CO}_2/dt$, —) deduced from the temperature profiles at pilot scale for natural convection (\circ) and forced convection (\bullet) with Carignan grape must.

difference was probably largely due to the inaccurate profile of the air temperature;

(2) the experimental and the predicted CO₂ production rate and temperature (Fig. 7), using both:

- the kinetic model (Malherbe et al., 2004) to calculate the progression of the CO₂ production rate from the initial must composition (sugar, assimilable nitrogen);
- the thermal model to calculate the changes in the must temperature from the estimation of the CO₂ production rate and the external temperature, considering both natural and forced convection.

The combination of the models accurately predicted both the fermentation kinetics (Fig. 7(a)) and the kinetics of the must temperature (Fig. 7(b)).

To assess the accuracies of the models, we tested the kinetic model alone by fermenting the same must at a constant temperature in a 1 L reactor (Fig. 8). The calculated and measured CO₂ production rates were very similar. This confirms the accuracy of the kinetic model including for grape must, as has already been demonstrated by Colombié et al. (2005). Combined with the results shown in Fig. 7, this also validates the thermal model.

Best simulation results for fermentation kinetics (especially the shape of the curve at the end of the fermentation, Fig. 7(a)) were obtained for natural convection. This is consistent with the 100 L tanks being indoors. Conversely,

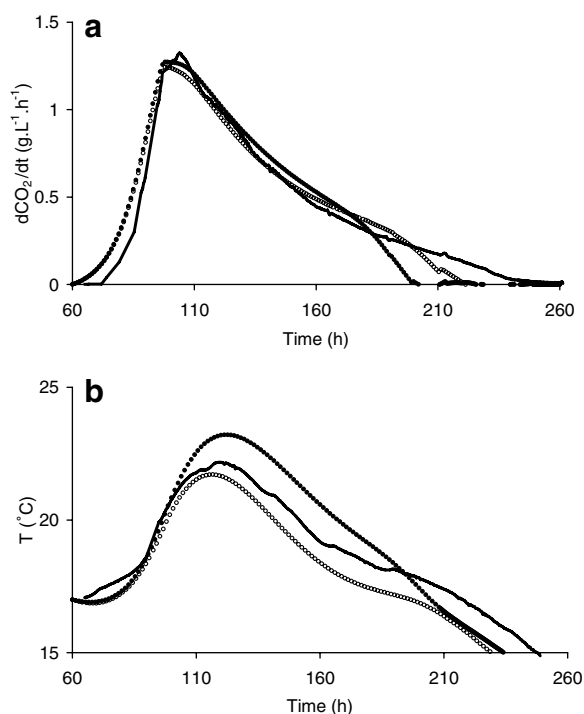


Fig. 7. Simulation of (a) the fermentation rate (dCO_2/dt , —) and (b) the must temperature (T , —) by the kinetic model including the heat transfer model for of natural convection (○) and forced convection (●). Experiment performed at pilot scale (100 l) with Carignan grape must.

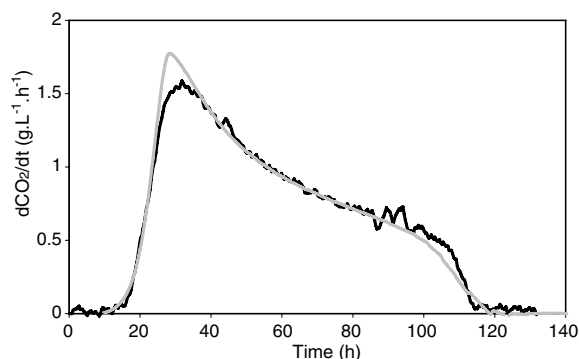


Fig. 8. Experimental fermentation rate (—) and the corresponding simulation with the kinetic model (---). Experiment performed at laboratory scale (1 l, $T = 24$ °C) with Carignan grape must.

at large scale for tanks located outside, forced convection is likely to give better simulation results than natural convection.

Although we did not test the thermal model in industrial conditions, we believe that it is applicable at this scale. In large tanks, the surface area to volume ratio is small and the loss of heat by convection represents only a small percentage of that produced by the fermentation (less than 10%). Pilot scale fermentations, used in our study, are much more discriminating conditions.

7. Conclusion

In this study, we developed a model to estimate the thermal behavior of tanks during wine fermentation. The model, combined with the kinetic model developed previously (Malherbe et al., 2004) was validated at the pilot scale. It can be used to estimate the power required to cool the fermentation tanks. The model can now be integrated into new control systems for wine making, for example to optimize the use of tanks and the energy required to cool the entire winery. This work is of particular interest for the design of cellars and can be used to optimize the size of the cooling systems.

Appendix. 1. Nomenclature

CO_2	carbon dioxide released (g L ⁻¹)
S	residual glucose concentration (g L ⁻¹)
S_0	initial glucose concentration in the must (g L ⁻¹)
dCO_2/dt	CO ₂ production rate (g L ⁻¹ h ⁻¹)
dT/dt	rate of must temperature change (°C h ⁻¹)
$P_{\text{accumulation}}$	power accumulated by the must (kcal h ⁻¹)
$P_{\text{fermentation}}$	power generated by the fermentation (kcal h ⁻¹)
P_{wall}	power exchanged by the walls of the tank (kcal h ⁻¹)
$P_{\text{evaporation}}$	power lost by evaporation of water and ethanol (kcal h ⁻¹)
Q_c	power withdrawn by the refrigeration system also called frigories (kcal h ⁻¹)

T_e	air temperature ($^{\circ}\text{C}$)
T	temperature of the must ($^{\circ}\text{C}$)
V	must volume in the tank (m^3)
ρ_{must}	must density (kg m^{-3})
Cp_{must}	specific heat capacity of the must ($\text{cal kg}^{-1} \text{ }^{\circ}\text{C}^{-1}$)
h_i	convection heat transfer coefficient inside the tank ($\text{cal h}^{-1} \text{ m}^{-2} \text{ K}^{-1}$)
h_e	convection heat transfer coefficient outside the tank ($\text{cal h}^{-1} \text{ m}^{-2} \text{ K}^{-1}$)
s_{air}	air speed (m s^{-1})
ν_{air}	air kinematic viscosity ($\text{m}^2 \text{ s}^{-1}$)
α_{air}	air thermal diffusivity ($\text{m}^2 \text{ s}^{-1}$)
λ_{air}	air thermal conductivity ($\text{cal h}^{-1} \text{ m}^{-1} \text{ K}^{-1}$)
λ	tank material thermal conductivity ($\text{cal h}^{-1} \text{ m}^{-1} \text{ K}^{-1}$)
A	heat transfer area (m^2)
r	radius of the tank (m)
e	thickness of the tank wall (m)
H	must height in the tank (m)
g	gravity (m s^{-2})
U	overall heat transfer coefficient ($\text{cal h}^{-1} \text{ m}^{-2} \text{ K}^{-1}$)

2. Data used for simulations

$T_e = 20 \text{ }^{\circ}\text{C}$; $V_{\text{must}} = 20 \text{ m}^3$; $r = 1.7 \text{ m}$; $H = 2.1 \text{ m}$; $e = 0.002 \text{ m}$, $s_{\text{air}} = 1.4 \text{ m s}^{-1}$; $g = 9.8 \text{ m s}^{-2}$
 $h_i = 25837 \text{ cal h}^{-1} \text{ m}^{-2} \text{ K}^{-1}$; $\lambda = 13750 \text{ cal h}^{-1} \text{ m}^{-1} \text{ K}^{-1}$
 $\nu_{\text{air}} = 1.4879\text{e}-5 \text{ m}^2 \text{ s}^{-1}$; $\alpha_{\text{air}} = 2.95\text{e}-5 \text{ m}^2 \text{ s}^{-1}$; $\lambda_{\text{air}} = 27.28 \text{ cal h}^{-1} \text{ m}^{-1} \text{ K}^{-1}$

References

- Bely, M., Sablayrolles, J.-M., & Barre, P. (1990). Description of the alcoholic fermentation kinetics: its variability and significance. *American Journal of Enology and Viticulture*, *41*, 319–324.
- Bouffard, A. (1895). Détermination de la chaleur dégagée dans la fermentation alcoolique. *Progrès Agricole et Viticole*, *24*, 345–347.
- Boulton, R. (1980). The prediction of fermentation behavior by a kinetic model. *American Journal of Enology and Viticulture*, *31*, 40–45.
- Colombié, S., Malherbe, S., & Sablayrolles, J. M. (2005). Modeling alcoholic fermentation in enological conditions: feasibility and interest. *American Journal of Enology and Viticulture*, *56*(3), 238–245.
- Dubrunfaut (1856). Note sur la chaleur et le travail mécanique produits par la fermentation vineuse. *Compte Rendu Académie des Sciences*, *42*, 945–948.
- El Haloui, N. E., Picque, D., & Corrieu, G. (1987). Mesures physiques permettant le suivi biologique de la fermentation alcoolique en oenologie. *Sciences des Aliments*, *7*, 241–265.
- Guymon, J. F., & Crowell, E. A. (1977). The nature and cause of cap-liquid temperature differences during wine fermentation. *American Journal of Enology and Viticulture*, *28*(2), 74–78.
- Le Roux, J. M. W., Purchas, K., & Nell, B. (1986). Refrigeration requirements for precooling and fermentation control in wine making. *South African Journal of Enology and Viticulture*, *7*, 6–13.
- Lienhard, J. H. (2000). In G. H. Lienhard (Ed.), *Heat transfer textbook* (3rd ed., pp. 392). Cambridge, USA: MIT Press.
- Lopez, A., & Secanell, P. (1992). A simple mathematical empirical model for estimating the rate of heat generation during fermentation in white wine making. *International Journal of Refrigeration*, *15*, 1–5.
- Malherbe, S., Fromion, V., Hilgert, N., & Sablayrolles, J. M. (2004). Modeling the effects of assimilable nitrogen and temperature on fermentation kinetics in enological conditions. *Biotechnology and Bioengineering*, *86*(3), 261–272.
- Manzocco, L., Maltini, E., & Lericci, C. R. (1998). Changes of some thermal and physical properties in model system simulating an alcoholic fermentation. *Journal of Food Processing and Preservation*, *22*, 1–12.
- MatéVi. Available from <http://www.matevi-france.com/>.
- Mc Adams, W. H. (1954). In W. H. Mc Adams (Ed.), *Heat transmission* (3rd ed.). New York, USA: McGraw-Hill.
- Perry's Chemical Engineer's Handbook, 6th ed., sec. 11–28 McGraw-Hill, New York, 1984.
- Sablayrolles, J.-M., Barre, P., & Grenier, P. (1987). Design of a laboratory automatic system for studying alcoholic fermentations in anisothermal enological conditions. *Biotechnology Techniques*, *1*, 181–184.
- Singh, R. P. (1982). Thermal diffusivity in food processing. *Food Technology*, *36*(2), 87–91.
- Vannobel, C. (1988). Refroidissement d'un moût en fermentation par évaporation naturelle d'eau et d'alcool. *Connaissance de la Vigne et du Vin*, *22*, 169–187.
- Varma, R. R. (1999). Heat transfer in unitanks. *Monatsschrift Brauwissenschaft*, 4–8.
- Williams, L. A. (1982). Heat release in alcoholic fermentation: a critical reappraisal. *American Journal of Enology and Viticulture*, *33*, 149–153.
- Williams, L. A., & Boulton, R. (1983). Modeling and prediction of evaporative ethanol loss during wine fermentations. *American Journal of Enology and Viticulture*, *34*, 234–242.